JOURNAL OF MATERIALS SCIENCE:MATERIALS IN MEDICINE 9 (1998) 213–219

Ageing behaviour in a dental low-gold alloy with high copper content

K. HAMASAKI[†], K. HISATSUNE*[†], K. UDOH[‡], Y. TANAKA[‡], Y. IIJIMA[†], O. TAKAGI[†]
[†]*Department of Preventive Dentistry, and* [‡]*Department of Dental Materials Science, Nagasaki University School of Dentistry, Nagasaki 852, Japan*

S. NARUSE
Tokuriki Honten Co. Ltd, Tokyo 101, Japan

Phase transformation behaviour in a dental low-gold alloy with high copper content during continuous heating was investigated by hardness tests, electrical resistivity measurements, X-ray diffraction, scanning and transmission electron microscopies. Two kinds of solution treatment conditions (at 873 K and 1073 K) followed by iced-brine quench, represented different ageing behaviours. Although subsequent anisothermal annealing produced same phase separation of face-centred cubic disordered and ordered (Cu_3Au) phases in both specimens, the specimen quenched from 1073 K had already been hardened by a spinodal decomposition. © *1998 Chapman & Hall*

1. Introduction

It is well known that gold-base alloys are one of the most useful materials in dentistry. Typical dental gold alloy consists of gold, copper, silver and minor additions [1]. The alloys can obtain the required strength by age-hardening associated with an ordered structure CuAu I [2–4]. Since a sudden rise in the price of gold in 1980, interest was transferred to low-gold from high-gold alloys. The formation of CuAu I phase also plays a most important role for the age-hardening in those low-gold alloys [5–7]. In commercial low-gold alloys, we can find a unique alloy with higher copper content, which may have a good castability. The additional copper content must produce a characteristic behaviour, which can be expected from the ternary phase diagram of Au–Ag–Cu [8]. However, there has been no report of age-hardening in such alloys. In order to promote low-gold alloys in a new concept, it is very important to have a greater understanding of the ageing behaviour in low-gold alloys with high copper content. The purpose of the present work has to elucidate the phase transformation behaviour in a dental low-gold containing higher copper by means of hardness tests, electrical resistivity measurements, X-ray diffraction (XRD), scanning and transmission electron microscopies (SEM and TEM).

2. Material and methods

The specimen used in the present work was a dental low-gold alloy with 45 wt% Au–24.5 wt % Ag–24.5 wt % Cu–5 wt % Pd–1 wt % Pt (KP200S, Tokuriki Honten Co. Ltd, Tokyo, Japan). Sheets 0.5 and 0.1 mm thick were prepared by alternate rolling and annealing for the hardness tests and for other experiments, respectively. These specimens were solution-treated at 873 or 1073 K for 3.6 ks and then quenched into ice–brine. Subsequently, anisothermal annealing was carried out at a heating rate of 1.67, 3.33, 8.33, 16.7 or 33.3 mK^{-1} s from room termperature to 1073 K *in vacuo*. The hardness tests were made using a diamond pyramid hardness identor with 300 g load. Each hardness value quoted is the average of five identations. The electrical resistivity measurements were made by using a potentiometric method [9]. The structural changes were examined with XRD, SEM and TEM. Specimens for the SEM observations were prepared by using a standard metallographic technique, with final etching achieved with a freshly prepared aqueous solution of 10% potassium cyanide and 10% ammonium persulphate. For the TEM study, discs of 3 mm diameter were punched out and subjected to appropriate annealing. Then these specimens were polished by ion beam (Precision Ion Polisher M691, Gatan Inc., USA). The electron microscopes used (S-430 nd H-800, Hitachi Co., Japan) were operated at 20 and 200 kV, respectively. The XRD study was carried out on the filed and appropriately heat-treated powder specimens by using nickel-filtered CuK_α radiation (RAD-rA, Rigaku Corp., Japan). Other experiments, except the resistivity, were made at room temperature in the specimens quenched from each temperature.

*Author to whom all correspondence should be addressed.

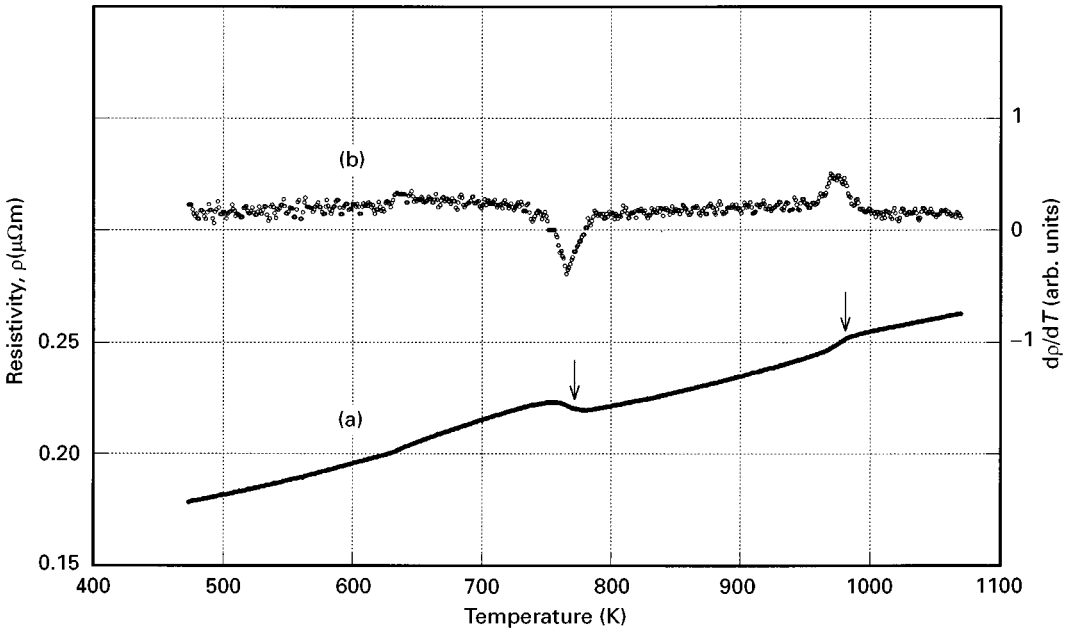

Figure 1 (a) Cooling curve of resistivity and (b) its temperature derivatives in a low-gold alloy at a cooling rate of 16.7 mK s^{-1}.

3. Results and discussion

3.1. Equilibrium phases

Fig. 1a shows a cooling curve of resistivity with a rate of 16.7 mK s^{-1}. In the vicinity of the temperatures indicated by arrows, some phase transformations must occur in the present alloy. This is more obvious in its temperature derivatives curves as shown by open circles in Fig. 1b. It is considered that the equilibrium phases were obtained in each temperature region, because the same types of behaviour were confirmed in cooling at the rates of 1.67–33.3 mK s^{-1}, although the data are not shown in Fig. 1. However, it is noted that the resistivity change is very strange for a phase transformation around 790 K, namely not a decrease but an increase in resistivity. Phase transformation is generally accompanied by a decrease in resistivity, though a similar characteristic has been reported on the formation of an ordered Au_3Cu phase with $L1_2$ structure [10, 11]. This will be discussed below.

The equilibrium phases were identified from XRD of the specimens during cooling at 16.7 mK s^{-1}. Fig. 2 shows variation of the XRD profiles. The specimen quenched from 1073 K produces α_0 single phase having a face-centred cubic (fcc) structure except for broad peaks near the fundamental reflection lines, as indicated by arrows, which will be discussed later. The lattice parameter was estimated to be $a = 0.390$ nm using the Nelson–Riley function [12]. At 873 K, two phases ($\alpha_1 + \alpha_2$) were detected. These were identified as fcc structures with $a_{\alpha 1} = 0.4053$ nm and $a_{\alpha 2} = 0.3831$ nm. At room temperature (298 K), two phases were confirmed as an fcc structure with

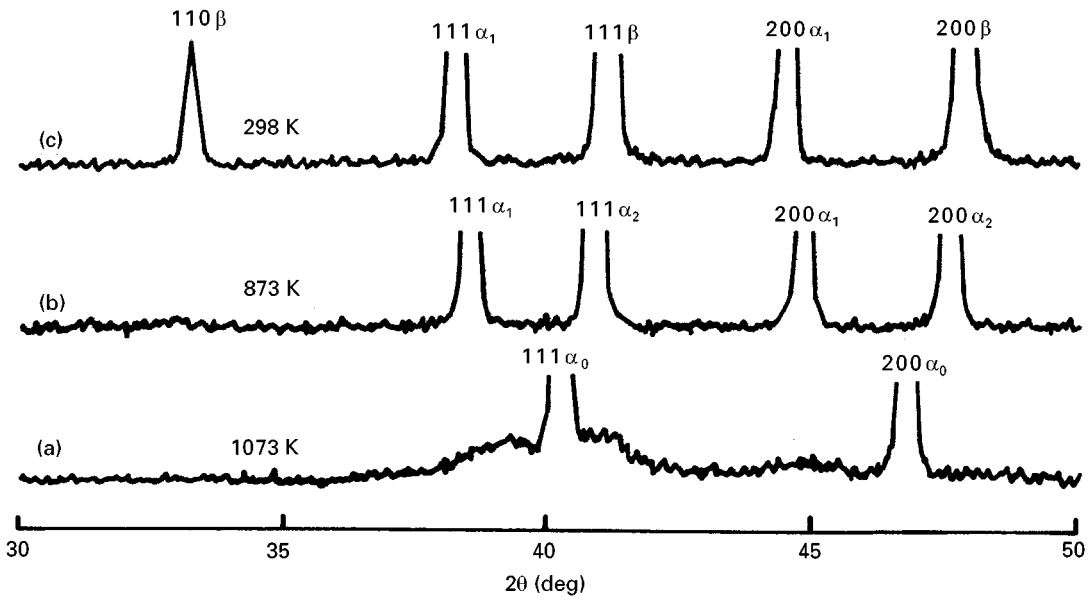

Figure 2 Variation of XRD profiles in the low-gold alloy quenched from (a) 1073 K, (b) 873 K and (c) 298 K on cooling at 16.7 mK s^{-1}.

$a_{\alpha 1} = 0.4080$ nm and an ordered fcc structure with $a_{\beta} = 0.3809$ nm. It is considered that this ordered phase is not Au_3Cu but Cu_3Au with $L1_2$ structure, judging from the fact that the lattice parameter is comparable with that of pure Cu_3Au (0.374 84 nm) [13] and the atomic ratio of Cu/Au is 1.7, which is located at a composition between CuAu and Cu_3Au. Moreover, Syutkina *et al.* [14] have reported an increment in the electrical resistivity of Cu_3Au alloy with palladium or platinum as the added third element. As pointed out for $CuAu_3$ by Hirabayashi [10], the resistivity increment may correspond to nucleation and growth of small anti-phase domains having a critical size for the scattering of electrons [15]. In any event, it was elucidated that the present alloy has three different equilibrium phase regions.

3.2. Electrical resistivity changes

The manufacturer of the present alloy recommends a temperature of 873 K for a solution treatment. However, this temperature is placed in a two-phase region as mentioned above. As a single-phase region should be generally selected, a temperature around 1073 K may be suitable in the present alloy. First, the ageing behaviour in the specimens with different solution-treatment temperatures were compared.

Fig. 3a shows anisothermal annealing curves of electrical resistivity, ρ, at a heating rate of 1.67 mK s^{-1} in the specimens with different solution-treatment temperature (873 and 1073 K). Normalized resistivity (ρ_T/ρ_{1073}) is a ratio of the resistivity at each temperature (TK) and that at a solution-treatment temperature (1073 K). As can be seen in the figure, four stages for phase transformation are confirmed. This behaviour is also clear in the temperature derivatives curves as shown in Fig. 3b. Stages I, II and III indicate decreases of the resistivity, while stage IV indicates a decrease in the slope. Resistivity change in stage I is remarkably different. It is noticed that the stage I in the specimen solution-treated at 1073 K occurred in lower temperature compared to that at 873 K. The resistivity begins to decrease at about 430 K and at about 520 K, respectively. It is obvious that the former (1073 K) is an easier reaction than the latter (873 K), as is also indicated by the value of the activation energy, see later. Stage II is more remarkable in the specimen solution-treated at 1073 K. It is considered that Stages III and IV correspond to the reactions to each equilibrium phase, judging from the XRD and resistivity data mentioned above.

Stage I is the main reaction in the present alloy, as shown later in hardness data. If the amount of reaction rate can be proportional to the change of resistivity, the reaction rate may correspond to the $d\rho/dT$ value. The reaction rate of each Stage I depended on the heating rate, although the data with another heating rate are not shown in Fig. 3. It is well known that there is a relationship, as shown below by Kissinger's equation [16], between the activation energy and the rate dependence

$$\mathrm{d}\left(\ln\frac{\Phi}{T_m^2}\right)\Big/\mathrm{d}\left(\frac{1}{T_m}\right) = -\frac{E}{R} \qquad (1)$$

where Φ is the heating rate, T_m the temperature at which the reaction rate attained a maximum value, E the activation energy and R the gas constant. Applying Kissinger's equation to this rate dependence, straight lines were obtained, as shown in Fig. 4. The activation energies are then calculated from the slope of each straight line. The apparent activation energies for Stage I in the specimens solution-treated at 873 K and 1073 K were 252.1 ± 32.0 and 142.7 ± 27.5 kJ mol^{-1}, respectively.

3.3. Age-hardening behaviour

Fig. 5 shows variations of hardness with temperature during continuous heating at a rate of 1.67 mK s^{-1}.

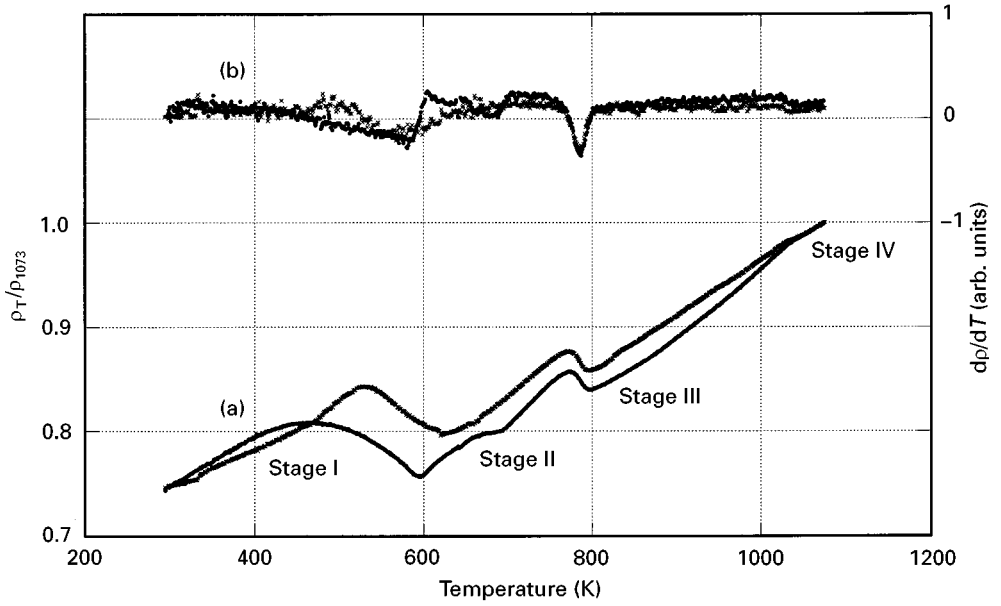

Figure 3 Anisothermal annealing curves of (a) resistivity and (b) their temperature derivatives in a low-gold alloy at two solution-treatment temperatures (×) 873 K and (●) 1073 K.

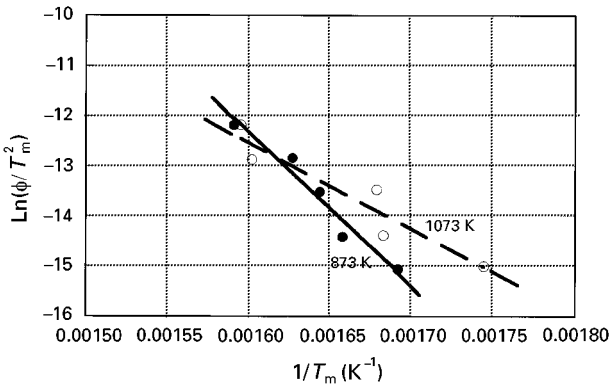

Figure 4 Application of Kissinger's equation for the main reaction in a low-gold alloy with two solution-treatment temperatures.

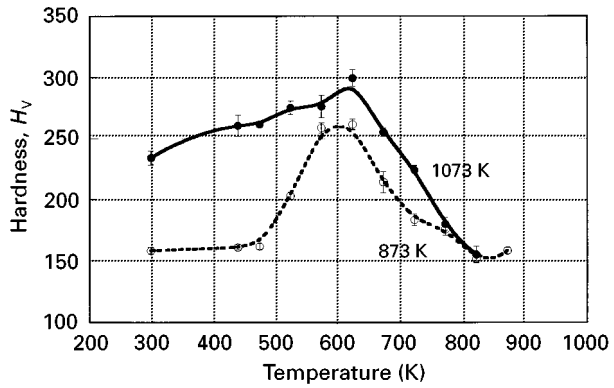

Figure 5 Variations of hardness with temperature during continuous heating at a rate of 1.67 mK s^{-1}.

Two kinds of solution-treatment temperature were employed. The hardness of the specimen solution-treated at 873 K begins to increase at about 500 K and attains a peak at about 600 K. Thereafter a softening occurs with increasing temperature. The temperature region that produced a remarkable hardening corresponds to that of Stage I. Stages II and III produced a softening.

On the other hand, the specimen solution-treated at 1073 K and quenched had already hardened before the subsequent annealing. It is implied that some phase transformation occurred during the quenching. Considering the purpose of solution treatment which should produce a softening state, it is reasonable that the manufacturer did not choose 1073 K as the solution-treatment temperature. Subsequent annealing produces an additional hardening. The hardness has already increased at 423 K and attains a peak at about 623 K, followed by a softening, as with solution-treatment at 873 K. It is obvious that a different hardening behaviour was produced, depending on the solution-treatment condition.

3.4. Ageing reactions

Fig. 6 shows the variation of the XRD profile in the specimen solution-treated at 873 K during continuous heating at a rate of 1.67 mK s^{-1}. As mentioned above, the as-quenched sample has two phases ($\alpha_1 + \alpha_2$) with f c c structure. As can be seen in the XRD profile at

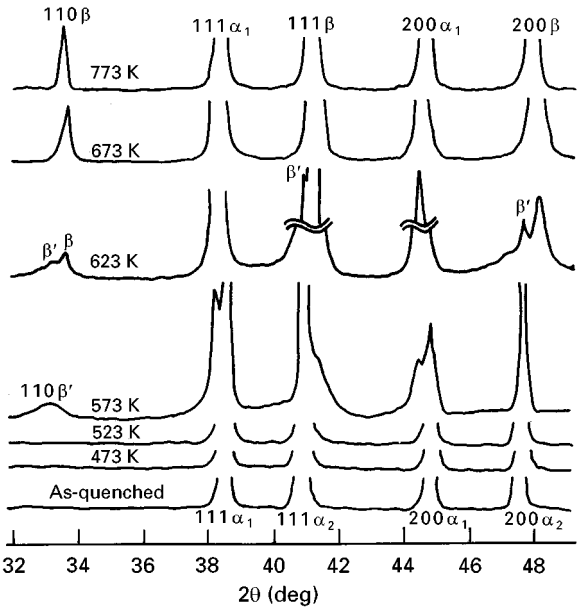

Figure 6 Variations of XRD profile during continuous heating at a rate of 1.67 mK s^{-1} in the specimen solution-treated at 873 K.

573 K which corresponds to Stage I, the fundamental reflection peaks of 1 1 1 and 2 0 0 for the α_1 and α_2 phases decrease in intensity and new peaks are detected. New phases were identified as an α_1' phase with f c c structure and a β' phase (Cu_3Au) with ordered f c c structure. The prime refers to a metastable phase. This stage corresponds to the main reaction which is attributed to the hardening. The apparent activation energy for this stage was 252.1 kJ mol^{-1}. Although there are no diffusion data in such a multicomponent system, the value obtained is close to an activation energy for self-diffusion in palladium or platinum [17].

With rising temperature, namely at 675 or 725 K, stable phases were produced. These were identified as the α_1 (f c c) and the β (Cu_3Au ordered f c c) phases. As can be seen in the XRD profile at 623 K, a coexistent state is confirmed, namely metastable (β') and stable Cu_3Au (β) phases. This is the first report of the coexistence of Cu_3Au in commercial dental alloys. This situation is analogous to what Hisatsune *et al.* [4–6] found in dental gold alloys. According to their reports, a metastable phase CuAu I′ was produced in the grain interior and contributed to the hardening, and further annealing yielded a stable phase CuAu I at the grain boundary. Fig. 7 shows (a) a selected-area diffraction pattern of the [1 0 0] zone, (b) its key diagram, (c) 0 1 0 (Cu_3Au) dark-field image, and (d) 2 0 0 (α_1') dark-field image in the specimen heated up to 623 K, at which a hardness peak was obtained. The diffraction analysis proves the formation of α_1' phase with f c c structure and β' phase with ordered f c c structure (Cu_3Au). Satellites around the fundamental spots could be interpreted as double diffraction. It is obvious that the dark-field images reveal a coexistent state of $\alpha_1' + \beta'$ in the grain interior. A nodular reaction (Stage III) to the stable phases ($\alpha_1 + \alpha_2$) which corresponds to softening, was confirmed by SEM observation, as shown in Fig. 8. The ageing reactions of the specimen

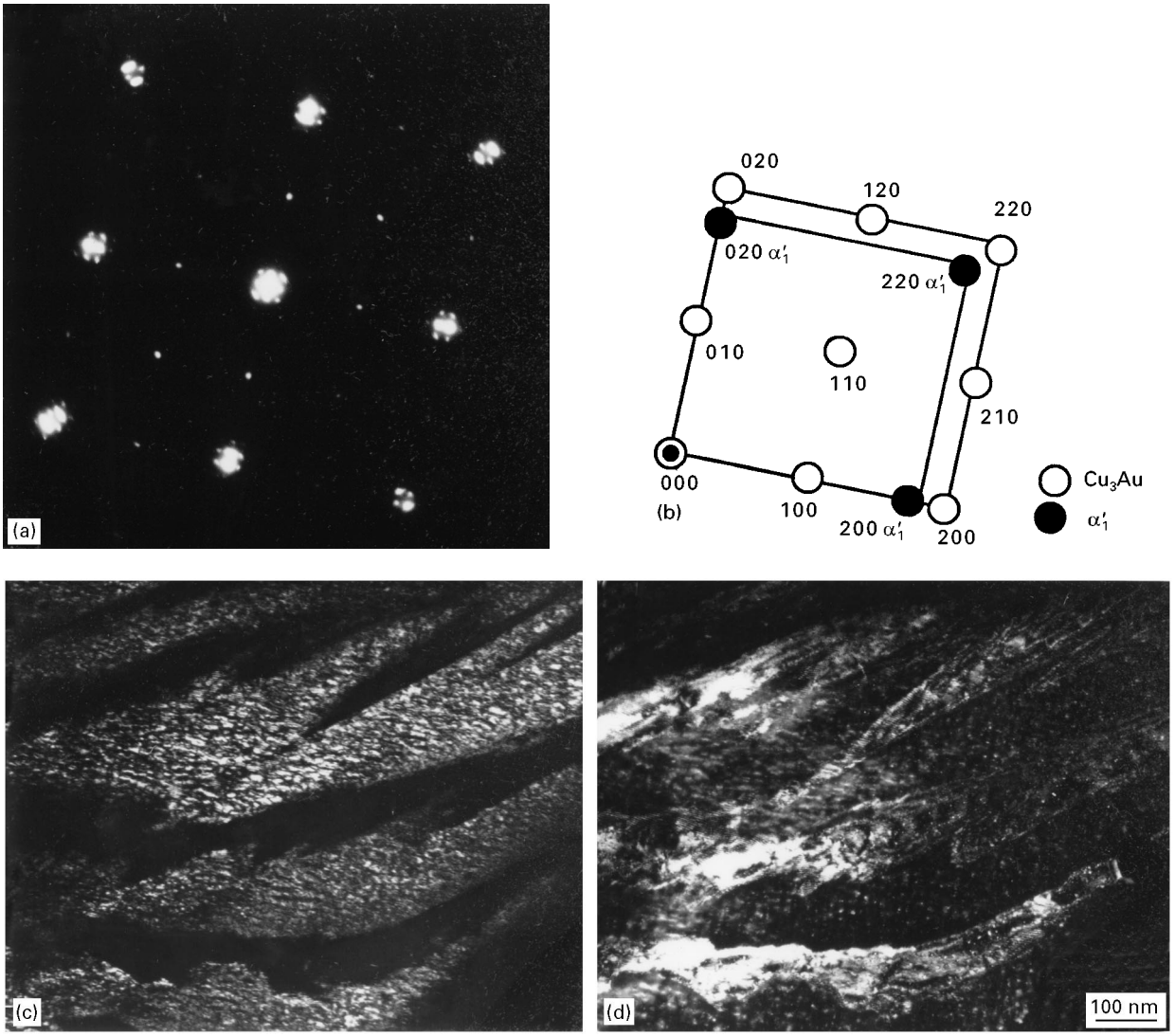

Figure 7 (a) Selected-area electron diffraction of the [0 0 1] zone, (b) its key diagram, (c) 0 1 0 dark-field image of the Cu_3Au phase, and (c) 2 0 0 dark-field image of the α_1' phase in the specimen heated to 623 K.

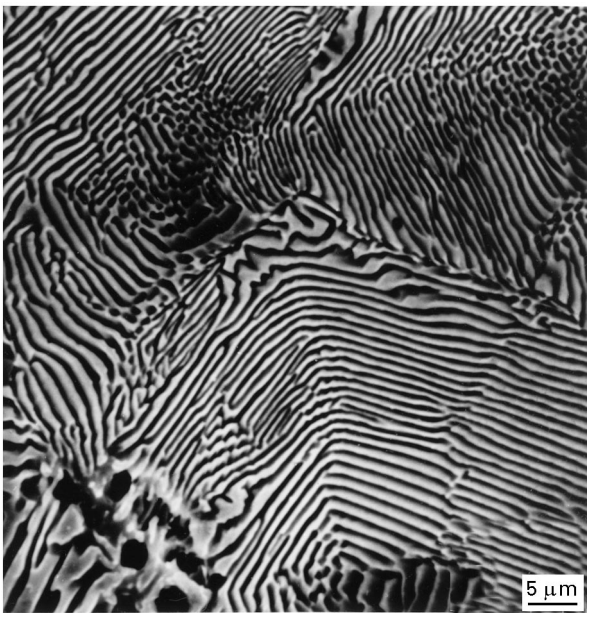

Figure 8 SEM image of the specimen heated to 823 K.

solution-treated at 873 K are characterized by the following sequence

$$\underbrace{\alpha_1 + \alpha_2}_{\text{Stage III}} \rightarrow \alpha_1' + \beta' \rightarrow \underbrace{\alpha_1 + \beta}_{\text{Stage III}}$$

Stage I Stage II

In the case of the specimen solution-treated at 1073 K, the same behaviour was produced except for Stage I as shown in Fig. 9. At first, it is noticed that as the quenched state is not the same. During quenching from 1073 K, some phase change occurs. The XRD pattern accompanied sideband reflection peaks on both sides of the fcc fundamental reflections, as shown by arrows in Fig. 9. A modulated structure (MS) developed by spinodal decomposition was observed in TEM image as shown in Fig. 10. It is considered that a spinodal decomposition based on the Ag–Cu binary system was produced, due to the increasing copper content in the gold alloy. This is the

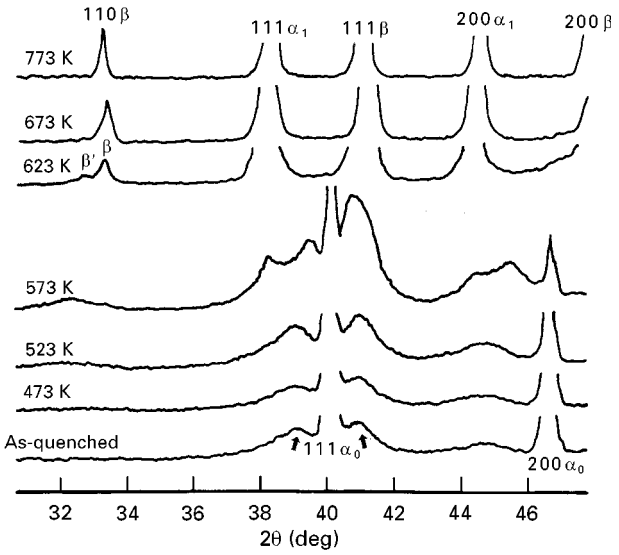

Figure 9 Variation of XRD profile during continuous heating at a rate of 1.67 mK s^{-1} in the specimen solution-treated at 1073 K.

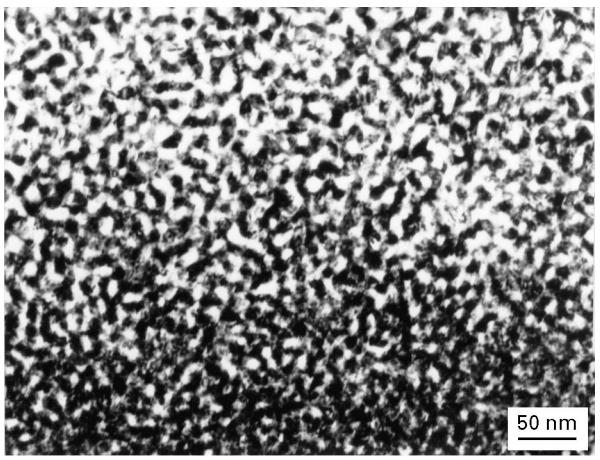

Figure 10 Bright-field image of the specimen quenched from 1073 K.

first report of spinodal decomposition in commercial dental gold alloys, although spinodal decomposition in the Au-Cu-Ag system has been found theoretically by Yamauchi *et al.* [18] and experimentally by Ohta *et al.* [19]. On increasing the temperature, the sidebands moved to the main line with increasing intensity and asymmetry in the sideband peaks. The wavelength of the MS was calculated from the angular distance between the sideband and the main peak, using the formula of Daniel and Lipson [20]. Fig. 11 shows variations of wavelength with temperature. The wavelength growth is observed with increasing temperature. The values are comparable with those reported by Ohta *et al.* [19] in Au–Cu–Ag ternary alloys. The hardening in the specimen quenched from 1073 K was caused by the coherency strain produced by a spinodal decomposition, as reported in a Fe–Mn–Al alloy by Sato *et al.* [21]. This stage was the main reaction for hardening during the continuous heating in the specimen quenched from 1073 K. The

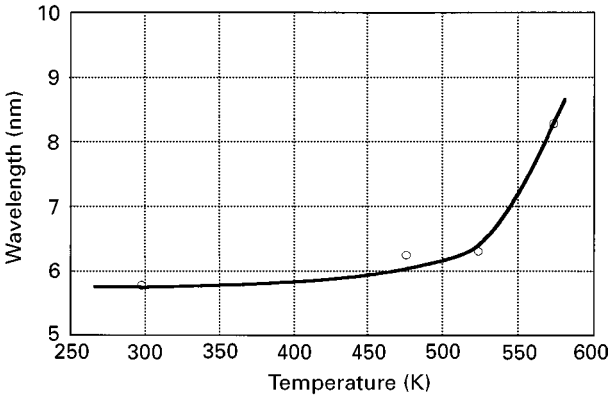

Figure 11 Variation of wavelength with temperature during continuous heating at a rate of 1.67 mK s^{-1} in the specimen solution-treated at 1073 K.

apparent activation energy for this stage was 142.7 kJ mol^{-1}. This value is very small compared to that in the specimen quenched from 873 K, that is, half of the activation energy for diffusion [17]. It is considered that the growth of the modulated structure was caused by the migration of quenched-in excess vacancies. In continuous heating after quenching, it is well known that the migration of quenched-in excess vacancies plays an important role in phase transformations [22, 23].

As mentioned in relation to resistivity changes, Stages II and III of the specimen solution-treated at 1073 K were similar to those at 873 K in the XRD profiles. Stage IV must correspond to an equilibrium phase change, namely from two fcc phases ($\alpha_1 + \alpha_2$) to a single fcc phase (α_0). The ageing reactions of the specimen solution-treated at 1073 K are characterized by the following sequence

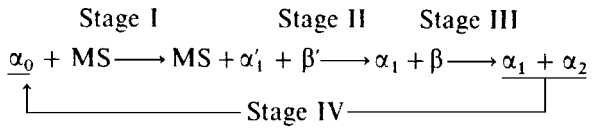

4. Conclusions

Ageing behaviour in a low-gold alloy containing a higher copper content was studied by hardness tests, electrical resistivity measurements, X-ray diffraction, scanning and transmission electron microscopies, The main results are as follows.

1. Three equilibrium phase regions, namely α_0(fcc), α_1(fcc) + α_2(fcc) and α_1(fcc) + β(Cu_3Au, $L1_2$) were confirmed.

2. The phase transformations proceeded in four stages during anisothermal annealing after solution-treatment.

3. A difference in the solution-treatment temperature followed by quenching produced a different hardening mechanism. At 873 K, the hardening was due to a precipitation of metastable Cu_3Au ordered phase with $L1_2$ structure, while spinodal decomposition contributed to the hardening at 1073 K.

References

1. R. W. PHILLIPS, "Skinner's Science of Dental Materials", edited by N.B. Saunders, (Philadelphia, PA, 1982), p. 374.
2. K. F. LEINFELDER, W. J. O'BRIEN and D. F. TAYLOR, *J. Dent. Res.* **51** (1972) 900.
3. A. PRASAD, T. ENG and K. MUKHERJEE, *Mater. Sci. Eng.* **24** (1976) 179.
4. K. HISATSUNE, M. NAKAGAWA, K. UDOH, B. I. SOSROSOEDIRDJO and M. HASAKA, *J. Mater. Sci. Mater. Med.* **1** (1990) 49
5. K. HISATSUNE, M. OHTA, T. SHIRAISHI and M. YAMANE, *J. Less-Common Metals* **83** (1982) 243.
6. *Idem*, *J. Dent. Res.* **61** (1982) 805.
7. K. HISATSUNE, K. UDOH, M. NAKAGAWA and M. HASAKA, *J. Less-Common Metals* **160** (1990) 247.
8. A. PRINCE, G. V. RAYNOR and D. S. EVANS, "Phase Diagrams of Ternary Gold Alloys" (The Institute of Metals, London, 1990) p. 7.
9. K. HISATSUNE, T. TANAKA, K. UDOH, A. M. EL ARABY, K. IWANUMA and K. YASUDA, *Dent. Mater. J.* **12** (1993) 233.
10. M. HIRBAYASHI, *J. Phys. Soc. Jpn* **14** (1959) 262.
11. P. WRIGHT and F. GODDARD, *Acta Metall.* (1959) 757.
12. J. B. NELSON and D. P. RILEY, *Proc. Phys. Soc.* (*Lond.*) **57** (1945) 160.
13. P. VILLARS and L. D. CALVERT, "Pearson's Handbook of Crystallographic Data for Intermetallic Phases", Vol. 2 (ASM, Metals Park, OH, 1986) p. 1198.
14. V. I. SYUTKINA, I. YE. KISLITSYNA, R. Z. ABDULOV and V. K. RUDENKO, *Phys. Met. Metall.* **61** (1986) 77.
15. N. F. MOTT, *J. Inst. Metals* **60** (1937) 267.
16. H. E. KISSINGER, *Anal. Chem.* **29** (1957) 1702.
17. Japan Institute of Metals "Metal Data Book", edited by S. Nagasaki, (Maruzen, Tokyo, 1974) p. 24.
18. H. YAMAUCHI, H. A. YOSHIMATSU, A. R. FOROUHI and D. DE FONTAINE, in "Proceedings of the 4th International Precious Metals Conference, edited by R. O. McGachie and A. G. Bradley, (Pergamon Press, Toronto, 1980) p. 241.
19. M. OHTA, T. SHIRAISHI, M. YAMANE and K. YASUDA, *Dent. Mater. J.* **2** (1983) 10.
20. V. H. DANIEL and H. LIPSON, *Proc. R. Soc. Ser. A* **181** (1943) 368.
21. K. SATO, K. TAGAWA and Y. INOUE, *Mater. Sci Eng.* **A111**(1989) 45.
22. K. HISATSUNE, *J. Jpn Inst. Metals* **42** (1978) 118.
23. K. MITSUI, Y. MISHIMA and T. SUZUKI, *Philos. Mag.* **A59** (1989) 123.

Received 2 April
and accepted 22 May 1997